Biomaterials 35 (2014) 4759–4768

Contents lists available at ScienceDirect

Biomaterials

journal homepage: www.elsevier.com/locate/biomaterials

A spatial patternable macroporous hydrogel with cell-affinity domains to enhance cell spreading and differentiation

Jing Sun, Dan Wei, Yuda Zhu, Meiling Zhong, Yicong Zuo, Hongsong Fan*, Xingdong Zhang

National Engineering Research Center for Biomaterials, Sichuan University, Chengdu 610064, Sichuan, China

ARTICLE INFO

Article history:
Received 23 December 2013
Accepted 21 February 2014
Available online 15 March 2014

Keywords:
Hydrogel
Cell adhesion
Cell spreading
RGD
Photocrosslinking
Osteon-like

ABSTRACT

Cell adhesion and spreading are two essential factors for anchorage-dependent cells such as osteocytes. An adhesive macroporous hydrogel system, in which cell-affinitive domains and sufficient cytoskeleton reorganization space were simultaneously constructed, was proposed in this report to support cell adhesion and spreading, respectively, and facilitate cell differentiation and function establishment eventually. The adhesive macroporous alginate hydrogel was developed by RGD peptide graft and gelatin microspheres hybridization to generate cellular adhesion sites and highly interconnected macropores. The successful stretched morphology and enhanced osteogenic differentiation of MG-63 cells in this modified alginate hydrogel showed clearly the feasibility that cell function may be effectively facilitated. Besides, this hydrogel model can be further applied to construct complex micropatterned structure, such as individual microgels in shapes of circle, square, cross and ring, and osteon-like structure containing both osteogenic and vascularized area generated by a double-ring assembly. These results should provide this adhesive macroporous photocrosslinkable hydrogel system as potential three-dimensional scaffolds for guiding tissue formation, especially for the bioengineering of tissues that have multiple cell types and require precisely defined cell–cell and cell–substrate interactions.

1. Introduction

The three-dimensional (3D) interaction between cells and extracellular matrix (ECM) constitutes a dynamic regulatory system for directing tissue formation and regeneration [1–3]. As such, significant progress has been made in engineering 3D hydrogels capable of promoting cell function and many of these important ECM interactions [4–6]. However, the inability to precisely control cell behavior has often resulted in poor cell and ECM organization within engineered constructs that had limited ability to recreate complex tissues [7,8]. Another important challenge is to control the spatial organization of cells in their synthetic microenvironments which is especially vital in the bioengineering of tissues that have multiple cell types and require precisely defined cell–cell and cell–substrate interactions [9,10]. Therefore, the spatial patterning of hydrogels in structure or chemical component, motivated by the microscale heterogeneity of native tissue architectures, has recently been the focus and nodus of advanced tissue engineering constructs to provide better control of cellular behavior [7]. Microgels fabricated by photomask-based stereolithography have been successfully integrated into the generation of complex structures with well-defined microarchitecture and enhanced control of cell behavior and function [11–13]. While a major challenge in the use of micro/macro-scaled hydrogel scaffolds is the settlement of cell spreading, migration and differentiation in 3D gel matrices [14].

Cell adhesion and spreading are two essential factors for anchorage-dependent cells such as osteocytes. The survival of these cells first requires attachment to a substrate, which relies on the interactions between receptors on cell surface and substrates, and determines the proliferation, differentiation and many other important cell behaviors [15]. As such cells require a stretched morphology to maintain their normal phenotype and function, the spreading is another indispensable factor for their subsequent settlement and commitment in 3D microenvironments [16,17]. Cell spreading is based on the accomplishment cell adhesion, successful cytoskeleton reorganization and, more importantly, it cannot do without the availability of space in 3D scaffolds [18]. Evidently, cell function cannot be performed without the successful cell adhesion and spreading. Unfortunately, both these cell behaviors could scarcely be achieved in common gel matrices due to the low cell

* Corresponding author. Tel.: +86 28 85410703; fax: +86 28 85410246.
E-mail address: hsfan@scu.edu.cn (H. Fan).

http://dx.doi.org/10.1016/j.biomaterials.2014.02.041
0142-9612/

affinity and high cell constraint [14]. Hence, much work has been focused on functionalizing 3D hydrogels to spatially and temporally control their internal cell adhesion and spreading.

One of the most common strategies is chemical modification with cell-affinitive domains such as Arg-Gly-Asp (RGD) or hybridization with cell-adhesive materials to provide integrin-binding sites to cells in the inert bulk of the hydrogel [6,19,20]. Another strategy, of which the central idea still focuses on the provision of cell-affinitive interfaces, is to physically hybridize functionalized microspheres or nanoaggregates into hydrogel bulk to support cell adhesion and stretching on their spherical surfaces [21–23]. Cells could survive and spread well within the composite, yet should be pre-seeded and cultured on the surface of the microspheres for several days to make a sufficient cell adhesion and spreading before encapsulating into the hydrogels. This increased the cumbersome nature of the process inevitably but, more important, the cell-laden microspheres can not be uniformly encapsulated into the hydrogel since vigorous mixing may cause cell shedding from the surface of the microspheres. Some other studies have mainly focused on the creation of space for cell proliferation and migration by relying on specific enzymatic digestion or hybridization of micro-porogens produced by the self-degradation of the microspheres as well as the photodegradable hydrogel which is another ingenious strategy [24–27]. But few can reach balance between enhanced cell–matrix interaction and the creation of spatial freedom for cell spreading, which accordingly resulted in the unfavorable functional expression and tissue ingrowth although cells encapsulated in the 3D hydrogels can spread to some extent. A typical example is the living hyaline cartilage graft developed by Dong-An Wang group via the strategy of phase transfer cell culture [28,29]. The chondrocytes encapsulated in alginate constructs were indicated to grow into the cavities created by the degrading gelatin microspheres, proliferate into colonies, and ultimately fill up the cavities. However, because of the intrinsic non-cell-adhesive property, this hybrid hydrogel system could not support anchorage-dependent cells stretching into their favorable morphology but only suit such spherical cells like chondrocytes, and accordingly cannot be successfully applied on bone tissue construct.

In this work, the simultaneous construction of both cell-affinitive domains and sufficient spreading space is emphasized in the design and modification of 3D hydrogel materials for the regeneration of tissues such as bone. We investigate the hypothesis that the incorporation of RGD peptide and macropores into inert hydrogel substrate, namely adhesive macroporous hydrogel system, which provide cellular adhesion sites and cytoskeleton reorganization space, will support cell adhesion and spreading, respectively, and facilitate cell differentiation and function establishment eventually. Here, the inert alginate, inherently non-adhesive, exhibited as the model hydrogel material; MG-63 was represented to investigate the proliferation, spreading and functional expression of such anchorage-dependent cells encapsulated in 3D hydrogel matrix. To produce the desirable adhesive macroporous alginate hydrogel, cellular adhesion peptide RGD was first grafted onto the alginate molecule chain to provide integrin-binding sites to MG-63 cells. Simultaneously, the macropores were created by the rapid degradation of the incorporated gelatin microspheres at 37 °C to generate space for cell spreading. Based on the adhesion ability and spreading space construct, we expected that anchorage-dependent cells such as MG-63 cells around spheres could spread and migrate gradually to the space left by the degraded microspheres on the premise of RGD involvement, and thus the prolonged cell survival and tissue growth in the artificial microenvironment were further facilitated. A schematic demonstration of cell spreading and proliferation in the construction of adhesive macroporous hydrogel is shown in Fig. 1A.

On the basis of the photocrosslinkable ability, microgels with different shapes, such as circle, square, cross and ring, were fabricated by this adhesive macroporous hydrogel model respectively. Moreover, by a two-step photolithography method, double-ring microgels with human umbilical cord vein endothelial cells (HUVECs) laded in the inner layer and MG-63 cells laded in the outer layer were assembled to generate osteon-like structure imitating Haversian system for bone-restructuring tissue engineering. Predictably, this adhesive macroporous hydrogel system, possessing spatial patterned ability and simultaneously enabling prolonged cell survival and differentiation, would have great potential applications for tissue engineering, especially for bottom-up macroscopic tissue engineering, realizing functional and spatially structured, complex, large-scale tissues.

2. Materials and methods

2.1. Materials

Sodium alginate was supplied by Fluka (item no. 71238) with a G/M ratio of 70/30. The cell adhesive oligopeptide GCGYGRGDSPG (MW: 1025.1Da) with >95% purity (per manufacturer HPLC analysis) were obtained from ChinaPeptides Co., Ltd. The UV light source (Omnicure S1500) was purchased from EXFO Photonic Solutions Inc. Gelatin, methacrylic anhydride, Irgacure 2959, Alexa Fluor-594 phalloidin, DAPI (4′,6-diamidino-2-phenylindole), FDA (fluorescein diacetate) and PI (propidium iodide) were obtained from Sigma–Aldrich. MTT (methyl thiazolyl tetrazolium) was obtained from Amreso (USA). All other chemicals were acquired from Chengdu Kelong Chem Co. unless otherwise specified.

2.2. Gelatin microspheres fabrication

Gelatin microspheres were prepared by an oil in water in oil (o/w/o) double emulsion method [21]. An aqueous solution (20 ml) of 10 wt% gelatin preheated at 70 °C was added to 10 ml of ethyl acetate. After vigorous stirring for 2 min with mechanical stirrer at 700 rpm, the mixture was quickly poured into 60 mL edible oil under agitation at the rate of 300 rpm for 1.5 min. The mixture was then transferred to a cool water bath and maintained at the same stirring rate for 15 min before pouring into ice-cold ethanol for 10 min. Gelatin microspheres were collected by washing with acetone to remove the residual edible oil. The washed gelatin spheres were air-dried and separated by standard sieve. Gelatin spheres with diameters of 100–150 μm were separated and utilized for preparation of microspheres hybrid alginate hydrogel.

2.3. Hydrogel preparation

The adhesive alginate hydrogels encapsulating gelatin microspheres were formed based on a previously described methacrylated alginate (MAA) hydrogel system with modifications. Briefly, MAA was synthesized through esterification of sodium alginate and methacrylic anhydride based on previously described protocols [30]. The methacrylation percentage of the MAA used in these experiments was roughly 50%. MAA was dissolved in a triethanolamine-buffered saline (TEOA buffer: 0.2 M TEOA, 0.3 M total osmolarity, pH 8.0) containing Irgacure 2959 photoinitiator (final concentration of 0.5 wt %). The cell adhesive peptide RGD dissolved in TEOA buffer was added to the MAA solution at a concentration consuming 10% acrylate groups on MAA based on the Michael-type addition chemistry, and allowed to react for 1 h at 37 °C before the hydrated gelatin microspheres (100–150 μm) were mixed. Following re-suspension of cells in this hybrid solution, the resultant homogenous blend was subsequently poured into molds and then exposed to 7.9 mW/cm^2 UV light (360–480 nm) for 20 s to allow free radical polymerization of MAA chains by photocrosslinking. Four microspheres containing hydrogels (AG0.5, AG0.75, AG1 and AG1.25) were prepared with an initial MAA concentration of 30 mg/ml and final volume ratio of gelatin microspheres/MAA = 0.5, 0.75, 1 and 1.25. The pure MAA hydrogel without gelatin microspheres (AG0) was prepared as control.

2.4. Hydrogel characterization

The mechanical properties of the hydrogels were characterized by compressive stress–strain measurements using an electromechanical universal testing machine (Model: CMT 4104) with a 200 N load cell (Shenzhen SANS Testing Machine co., LTD.). The cylindrical gel sample, 8 mm in diameter and 2 mm in thickness, was tested at a strain rate of 0.3 mm/min. The elastic modulus was determined by the average slope of the stress–strain curve over the strain range 0–25%. Three parallel samples per measurement were performed, and the obtained values were averaged.

The effect of gelatin microsphere incorporation on hydrogel swelling and rate of dissolution was investigated through swelling studies. Hydrogels without gelatin (AG0) and encapsulating gelatin microspheres (AG0.5 ~ 1.25) were formed as described above and the initial wet weight (Wo) was obtained after 24 h gelation. Hydrogels were then incubated in PBS at 4 °C for 24 h, and then half of the hydrogels

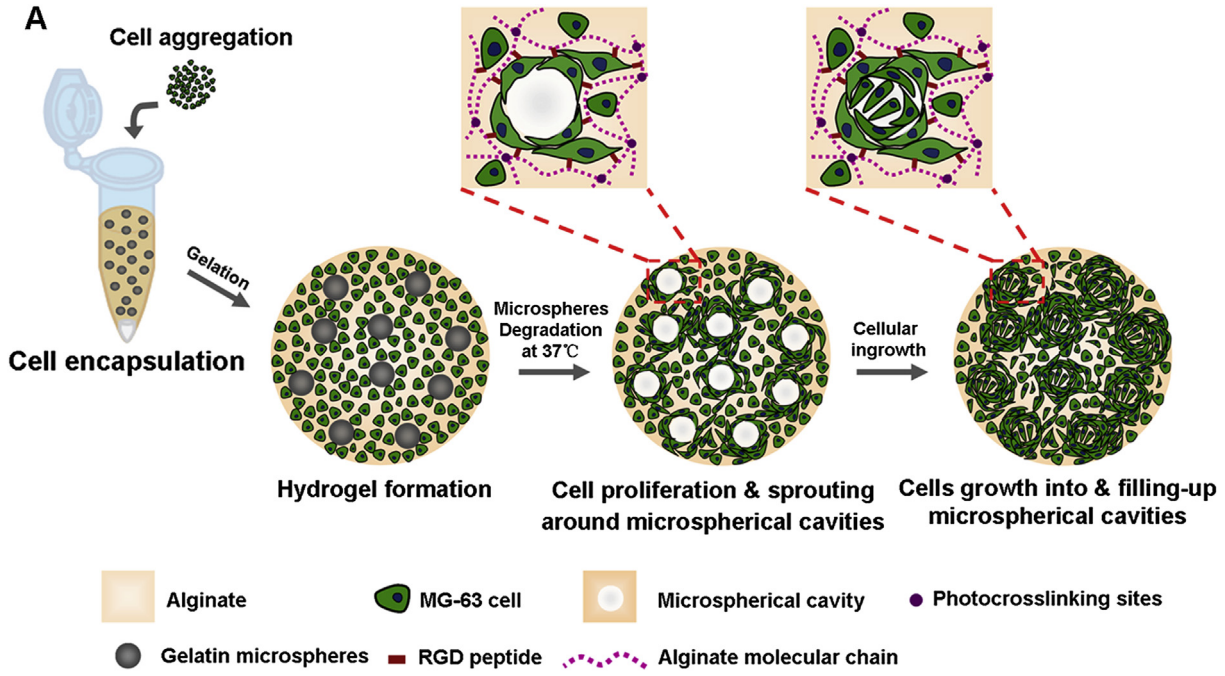

B

Composition of hydrogels and their nomenclature

Sample	The final MAA concentration (mg/mL)	RGD concentration	The final volume ratio of gelatin microspheres/MAA
AG0	15	0	0
RGD-AG0	15	10%	0
AG1	15	0	1:1
RGD-AG1	15	10%	1:1

Fig. 1. Preparation of RGD grafted macroporous alginate hydrogels. (A) Schematic demonstration of cell spreading and proliferation in the construction of adhesive macroporous alginate hydrogel. (B) Composition of hydrogels and their nomenclature.

were transferred to 37 °C to facilitate gelatin dissolution and the remaining hydrogels were stored at 4 °C to prevent gelatin dissolution. Wet weight (W) during immersion experiment was recorded at designated times. The swelling ratio was defined as $(W - Wo)/Wo$. Samples were tested in groups of three. Averages and standard deviations are reported. To evaluate the degradation of gelatin microspheres encapsulated within hydrogels, AG1 was taken as an example. The rhodamine-labeled gelatin (red) was employed to trace the dissolution of spheres and the residual gelatin in the construct after incubation in PBS at 37 °C was quantified from fluorescence images. At least six images for each sample were used for quantification of microspheres degradation.

2.5. Cell culture

The human MG-63 osteoblasts (ATCC, USA) and human umbilical cord vein endothelial cells (HUVECs) were cultured in Dulbecco's modified Eagle's medium (DMEM, Hyclone) supplemented with 10% fetal bovine serum (FBS, Hyclone), 1% penicillin/streptomycin (Hyclone) at 37 °C in an atmosphere with 100% humidity and 5% CO_2. The complete medium was replaced every 2–3 days and the cells were passaged twice a week when confluence was reached.

2.5.1. Cell encapsulation

For encapsulation studies, MG-63 cells were trypsinized, counted and resuspended in each hydrogel prepolymer at a density of 1×10^7 cells per mL. Cell containing blends were injected into molds and then exposed to 7.9 mW/cm^2 UV light (360–480 nm) for 20 s to gelate with certain shape and size. Composition of hydrogels used for cell encapsulation and their nomenclature was detected in Fig. 1B.

2.5.2. Cell proliferation

The MTT assay was used to count MG-63 cells after being cultured in the hydrogels. Cells encapsulated in samples gelating with 50 μL prepolymer solutions were incubated with 0.5 mg/ml MTT for 4 h at 37 °C. The solution was then removed and purple formazan salts dissolved with dimethyl sulphoxide, and the absorbance of the resulting solution was measured at 490 nm using a multidetection microplate reader (Bio-Rad 550).

2.5.3. Cell morphology in the hydrogels

Cell-laden hydrogels were stained with FDA/PI and visualized with a confocal laser scanning microscope (CLSM, Leica-TCS-SP5) to investigate the proliferation, distribution, and morphology of MG-63 cells. For actin cytoskeleton staining, the cell-laden gels were washed three times in DPBS and fixed in 4% paraformaldehyde solution in PBS for 5 min. After rinsed in PBS, 50 μg/mL Alexa Fluor-594 phalloidin was added to the samples to stain the actin cytoskeleton following 45 min incubation at room temperature. The samples were then rinsed in PBS and incubated in 0.1% (v/v) DAPI solution for 10 min to stain the nuclei, after which the samples were washed three times in PBS for confocal imaging.

2.5.4. Alkaline phosphatase activity

The activity of intracellular alkaline phosphatase (ALP) was measured with a SensoLyte pNPP Alkaline Phosphatase Assay Kit (AnaSpec, Inc.). Aliquots of 500 μL of cell lysate were obtained according to the procedure described for proliferation measurements and mixed with an equal amount of pNPP working solution in 96-well microplate. Mixtures were then incubated for 30 min at 37 °C. The reaction was stopped by the addition of 50 μL of stop solution to each well and the resulting

optical densities were measured at 405 nm with a μQuant spectrophotometer (Bio-Tek Instru-ments Inc., USA). Measurements were compared to alkaline phosphatase standard and normalized using the total protein amounts which were measured with a BCA protein assay kit (Pierce, USA).

2.5.5. Gene expression

At predetermined time points, total RNA was isolated from MG-63 cells using Trizol reagent (Invitrogen). RNA extracts were converted into complementary DNA (cDNA) using a reverse transcriptase polymerase chain reaction (RT-PCR) kit (ToYoBo, Japan). Quantitative real-time RT-PCR was performed by FTC-2000 Real-Time Fluorescence Quantitative Thermocycler (FungLyn Biotech Corp. Ltd, Shanghai, China). The sequences of primers for core-binding factor α1 (Cbfa1), bone morphogenetic protein-2 (BMP-2), collagen I (COL-I), osteocalcin (OCN) and glyceraldehyde-3-phosphate dehydrogenase (GAPDH) genes are given in Table 1. Amplification reactions were performed with a SYBR PrimeScript RT-PCR kit (Takara). The mRNA expression level of Cbfa1, BMP-2, Col-I, OCN and GAPDH was expressed as threshold cycle (CT) values, and the expression of the housekeeping gene GAPDH was used as internal control to normalize results. The comparative Ct-value method was used to calculate the relative expression. All samples were analyzed in triplicate.

2.6. Micropatterned hydrogels fabrication and osteon-like structure construct

To prepare cell-laden micropatterned hydrogel constructs, one droplet of the prepolymer cell suspension was pipetted between a PDMS (SYLGARD® 184, Dow Corning) coated glass slide and a TMSPMA treated glass slide separated by 300 μm high spacers. Subsequently, a photomask was placed on the top slide and microgels formation was induced by exposing the prepolymer to 7.9 mW/cm^2 UV light (360–480 nm) for 20 s. Immediately after polymerization, the top slide was removed and the remaining unpolymerized prepolymer cell suspension was gently washed away with PBS. Micropatterned cell-laden hydrogels were cultured for up to one week in 6-well-plates (Fisher Scientific) under standard culture conditions with the media exchanged every 3 days.

For osteon-like structure construct, the inner circular microgels with HUVECs encapsulation were first formed as mentioned above. The glass slide with the microgels was then placed on another prepolymer solution containing MG-63 cells, and a relevant photomask covering the inner-circle part was placed on the slide. Then, the solution was exposed to UV light for 20 s to generate the outer layered circle microgels. The double-layered circular microgel arrays with both HUVECs and MG-63 cells containing were then separated from the glass slide and manually assembled into a hollow tubular structure stabilized by 5 s of UV lighting. To test the connectivity of the channel within osteon-like microgel assemblies, Nile Red dye solution was perfused into the channel and the distribution image of the dye was observed under fluorescent microscopy (Leicactr 4000).

2.7. Statistical analysis

All results were expressed as mean ± standard deviation, and a paired Student's *t*-test was used to test for statistical significance between two types of samples. $P < 0.05$ was considered to be statistical significance.

3. Results

3.1. Mechanical testing

The mechanical properties of the hydrogels are presented in Fig. 2. With the incorporation of gelatin microspheres, the compressive modulus of the hydrogel was much higher than that of the pure photocrosslinked alginate hydrogel (AG0, ~68 kPa) except a comparable level between AG0.5 and AG0. The compressive modulus of the microspheres containing hydrogels increased significantly with the microspheres amount when the volume ratio of added microspheres was less than 1:1. However, with the continue increase of microspheres, the compressive modulus of AG1.25 decreased.

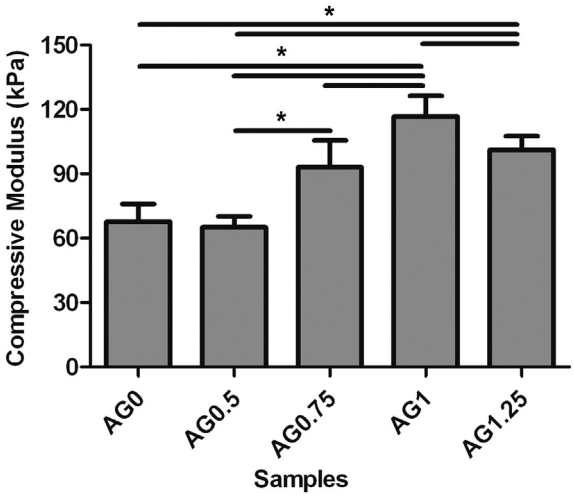

Fig. 2. The compressive modulus of the hydrogels. The compressive modulus of hydrogels increased significantly with the microspheres amount but somewhat decrease was detected in AG1.25 (*$p < 0.05$).

Table 1
Primers sequences for target genes.

Symbol	Primers
GAPDH	5′-GCCAAGGCTGTGGGCAAGGT-3′
	5′-AGGTGGAGGAGTGGGTGTCG-3′
Core binding factor α1	5′-CTCTACTATGGCACTTCGTCAG-3′
	5′-GCTTCCATCAGCGTCAACAC-3′
Bone morphogenetic protein-2	5′-TTACTGCCACGGAGAATGCC-3′
	5′-CCCACAACCCTCCACAACCA-3′
Collagen type I	5′-CACACGTCTCGGTCATGGTA-3′
	5′-AAGAGGAAGGCCAAGTCGAG-3′
Osteocalcin	5′-GAGGGCAGCGAGGTAGTGAA-3′
	5′-CCTCCTGAAAGCCGATGTGGT-3′

3.2. Swelling experiments

The swelling kinetics of the hydrogels in PBS at 4 °C and 37 °C is depicted in Fig. 3. When incubated in PBS at 4 °C, the swelling ratio of all the samples showed no apparent variation with incubation time and decreased with the incorporation of microspheres in a dose dependent manner. While for the hydrogels incubated in PBS at 37 °C, the swelling ratio also exhibited a decreased tendency with the increasing amount of microspheres, but the value changed with time because gelatin would degrade gradually at 37 °C. A rapid swelling occurred during the early incubation of 2 days, and then the swelling tendency slowed and dropped down after 4 days. For AG0 control, without gelatin encapsulation, the swelling ratio maintained a relatively higher level compared to other groups and changed very little with incubation time just as incubated at 4 °C.

3.3. Gelatin degradation

As shown in Fig. 4, the decreased number of rhodamine-labeled gelatin microspheres indicated that microspheres encapsulated in hydrogel AG1 dissolved gradually with incubation, and the degradation percentage after 3 days as shown in the statistical result was 90 ± 2%, indicating the majority of gelatin was degraded. The gradually blurred outline of the microspheres in the inserted light micrographs also illustrated the continuous dissolution of gelatin.

3.4. Cell proliferation

The MTT assay was implemented to quantitatively investigate the viability of MG-63 cells encapsulated in photocrosslinked alginate based hydrogels with and without gelatin microgels. As shown in Fig. 5, cells cultured in the hydrogels presented successively increasing viability in the order of AG0, RGD-AG0, AG1 and RGD-AG1 on the same day, except for the almost equal or slightly higher level in RGD-AG0 than cells in AG1 after 5 days in culture. For RGD-AG1, cells proliferated dramatically on day 3, after which cell viability maintained stable in the later culture time but still the

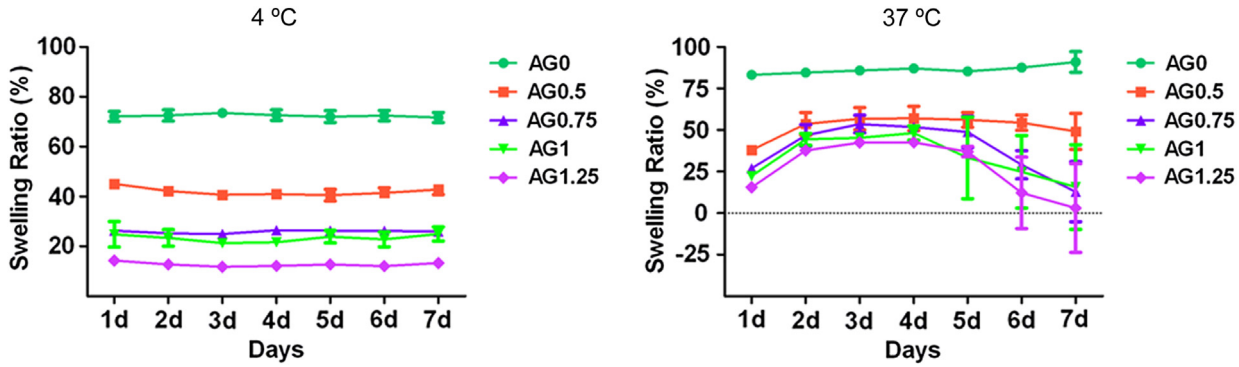

Fig. 3. The swelling properties of the hydrogels in pH 7.4 PBS at 4 °C and 37 °C. The swelling ratios of the hybrid hydrogels decreased significantly with the amount of gelatin microspheres and were much lower than control A1G0 (*$p < 0.05$).

highest among all the materials. In contrast, cells cultured in AG0 showed relatively lower viability as compared with those in other samples and there was no significant difference in cell proliferation until 10 days later. Encapsulated in RGD-AG0, cell maintained a steady proliferation and showed an equal level of cell viability with AG1 after 3 days culture, even outstripped the value of AG1 on the tenth day.

3.5. Cell morphology

FDA/PI staining and DAPI/F-actin staining were used to investigate the proliferation, distribution, and morphology of MG-63 cells encapsulated in hydrogels. As shown in Fig. 6A, cells in AG0 control sample remained a rounded morphology with a slow proliferation rate during the entire test period, only several cell clusters formed after 7 days. In contrast, some of the cells encapsulated in sample RGD-AG1 had started to form extensions around the microspheres after 1-day encapsulation, indicating that the cells were starting to spread. Subsequently, with the microspheres gradually degraded, the surrounding cells gradually grew into and eventually filled up the space left by microspheres degradation. Typical spindle shapes with tapering ends which indicated completely spread cell morphology had been developed for cells in RGD-AG1. Besides, the number of spreading cells in the RGD-AG1 hydrogel had visually increased, and direct cell–cell contact between spreading cells could be seen clearly by 5 days culture. For AG1, embedded with gelatin microspheres but without RGD containing, cells proliferated slowly around microspheres and the spreading was limited although cell aggregations were formed after 7 days. Similarly, cells in RGD-AG0 containing cell adhesion sites only, can spread and appeared protruding pseudopods, but the proliferation and the stretched morphology was still very restricted due to the lack of adequate space required for cell spreading. Cytoskeleton was observed more clearly by DAPI/F-actin staining (Fig. 6B), results revealed that cells in RGD-AG1 presented obvious cell spreading phenomenon even on the third day and the completely spreading was achieved after 5 days. While in the samples containing only microspheres or RGD peptide, cells could just exhibit a limited degree of spreading; either the spread cell number or the spreading degree was far beneath RGD-AG1 although certain improvement was gained along with culturing.

3.6. Alkaline phosphatase activity

Cell differentiation in the various hydrogels was characterized using ALP as an early osteogenic marker (Fig. 7). The ALP expression of cells in both RGD-AG1 and AG1 displayed a gradual rise with a peak at around day 14 and then decreased on day 21. Cells in RGD-AG1 remained the highest lever among all the four samples throughout the culture, whereas the ALP expression in AG0 was

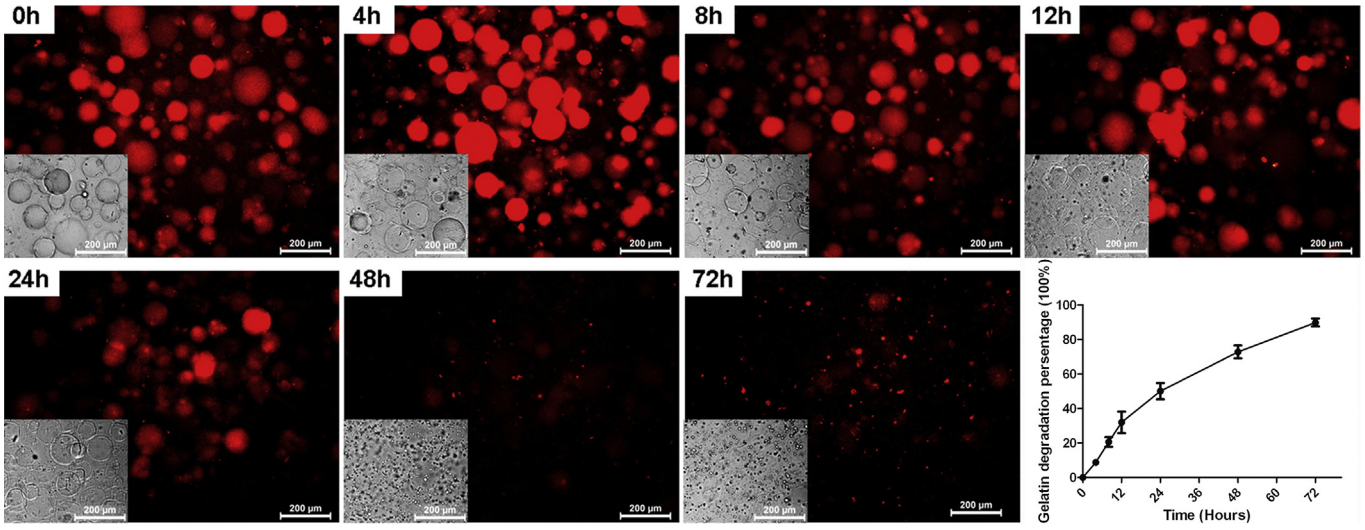

Fig. 4. Fluorescent photographs of rhodamine-labeled gelatin microspheres in sample AG1 after incubation in PBS at 37 °C over 3 days, from which the degradation kinetics of microspheres was quantified (lower right). Inset: light micrographs of gelatin microspheres in AG1 hydrogel.

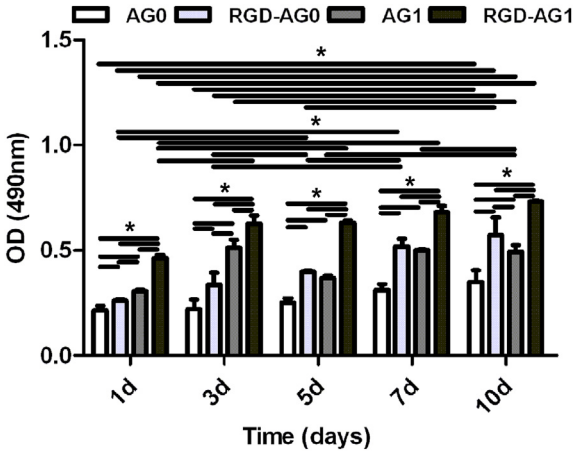

Fig. 5. MTT analysis of the MG-63 cells encapsulated in the hydrogels. Cells in RGD-AG1 showed statistically higher viability compared to other samples while cell viability in AG0 maintained a relatively lower value throughout the entire culturing ($^*p < 0.05$).

lowest and remained at the original lever over the entire test period. Regardless of day 4, ALP activity was somewhat higher at the same time point in AG1 as compared to RGD-AG0, in which ALP activity was decreased with the culture.

3.7. Osteogenic gene expression

Osteogenic differentiation of the MG-63 cells cultured in hydrogels was evaluated by the real time analysis of gene expression of Cbfa1, BMP-2, COL-I and OCN (Fig. 8). There was no significant difference in the levels of cbfa1 expression among all the samples at week 1. After that, the Cbfa1 mRNA expression increased dramatically in RGD-AG1 and AG1, especially a much higher expression was found in RGD-AG1. While in AG0 and RGD-AG0, a low cbfa1 expression was observed over the entire culture and no statistical difference was found between each other. The COL-I expression of MG-63 cells in RGD-AG1 showed a similar increasing trend to Cbfa1, while in the other samples, its increased expression did not occurred until 3 weeks later in a much lower level than RGD-AG1. For BMP-2 expression, the highest expression in RGD-AG1 was found at week 2, and then the expression dropped to a level even lower than that of AG1 at week 3. The OCN expression in RGD-AG1 showed a statistically much higher level than that in RGD-AG0 at the same time point and exhibited a significantly increase after culturing for 3 weeks, while the expression in AG0 and RGD-AG0 maintained a very low level throughout the culturing and no significant difference was found between each other.

3.8. Micropatterned hydrogels fabrication and osteon-like structure construct

Microgels with different shapes, such as circle, square, cross and ring, were fabricated respectively (Fig. 9A). MG-63 cells in these micropatterned hydrogels maintained a high activity and achieved a successful spreading after 7 days culture. By a two-step photolithography method, double-ring microgels with HUVECs laded in the inner layer and MG-63 cells laded in the outer layer were fabricated and assembled to generate osteon-like structure imitating Haversian system for bone-restructuring tissue engineering (Fig. 9B). The obtained double-ring microgel was showed to be tightly coupled and coaxial symmetric between inner and outer ring (Fig. 9C, D). A double-layered hollow tubular osteon-like structure was successfully constructed by the microgels assembly (Fig. 9E). After 4 days culturing, both HUVECs and MG-63 cells in the construct kept a high cell viability (Fig. 9F), and the microchannels were still connective as shown by the perfusion result (Fig. 9G).

4. Discussion

Engineered tissues designed to mimic native tissues must recreate the complex 3D cellular distribution and organization found in vivo, while maintaining the cell viability and function of the emulated tissues. Photopolymerized microgels with multitype cells patterning fabricated by photomask-based stereolithography

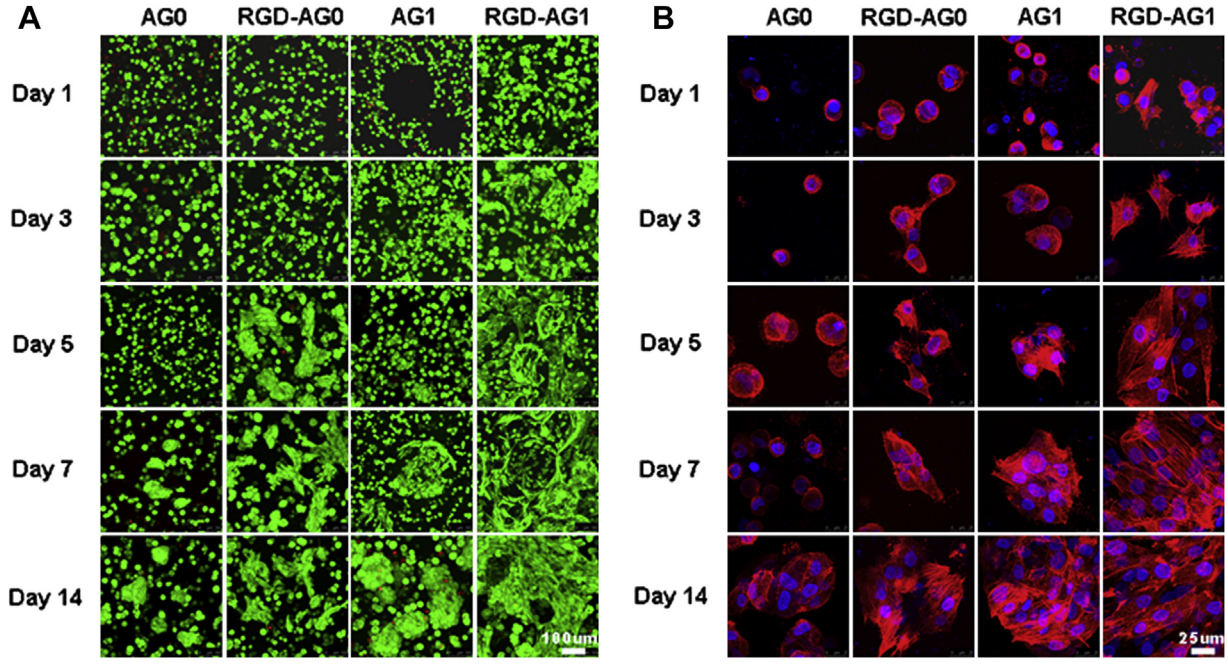

Fig. 6. Confocal microscopy images of MG-63 cells encapsulated in various hydrogels with (A) FDA/PI staining and (B) DAPI/F-actin staining.

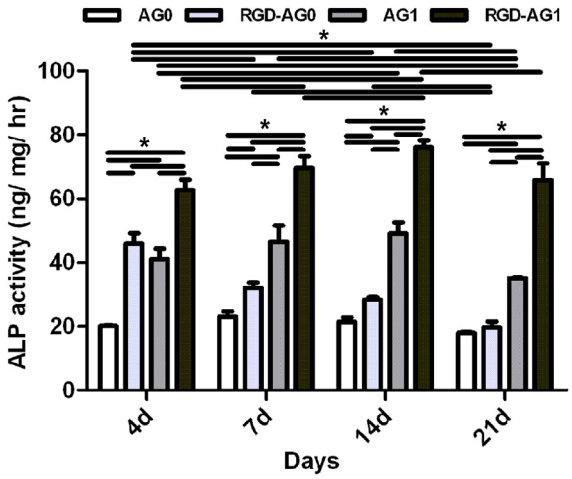

Fig. 7. Alkaline phosphatase expression of MG-63 cells during the 3 weeks of culture, normalized by DNA. The ALP expression of cells in RGD-AG1 increased remarkably with culture time on the first 14 days and then decreased significantly on day 21 ($^*p < 0.05$). However, the expression of the A1G0 control remained at a low level over the entire culture period.

meet this requirement successfully, while a major challenge of using micro/macro-scaled hydrogel scaffolds is the settlement of cell spreading, migration and differentiation in 3D gel matrices. Since the stretched morphology is extremely important to the survival and function of anchorage-dependent cells, the adhesive macroporous hydrogel system, in which cell-affinitive domains and sufficient spreading space were simultaneously constructed, was proposed in this report. Alginate hydrogels with RGD modified using a gentle Michael-type addition chemistry were made macroporous by the degradation of encapsulated gelatin microspheres at 37 °C. As shown in Fig. 1A, the integrin-binding site is first provided by the RGD peptide grafted on the MAA molecule chain to enhance the adhesion of MG-63 cells, so as to further facilitate cell survival and growth in the artificial microenvironment by the spreading space creation attributed to the degradation of gelatin microspheres incorporated in the hydrogel.

With the incorporation of gelatin microspheres, the hybrid alginate hydrogels exhibited significantly enhanced mechanical properties (Fig. 2) and decreased swelling ratios (Fig. 3). However, some decrease of the compressive modulus occurred when the volume ratio of added microspheres was very high (i.e., AG1.25), and the hydrogel collapsed after 6 days incubation (date was not shown) resulted in a sharp decline in gel weight. This is probably due to that an excessive amount of gelatin microspheres added

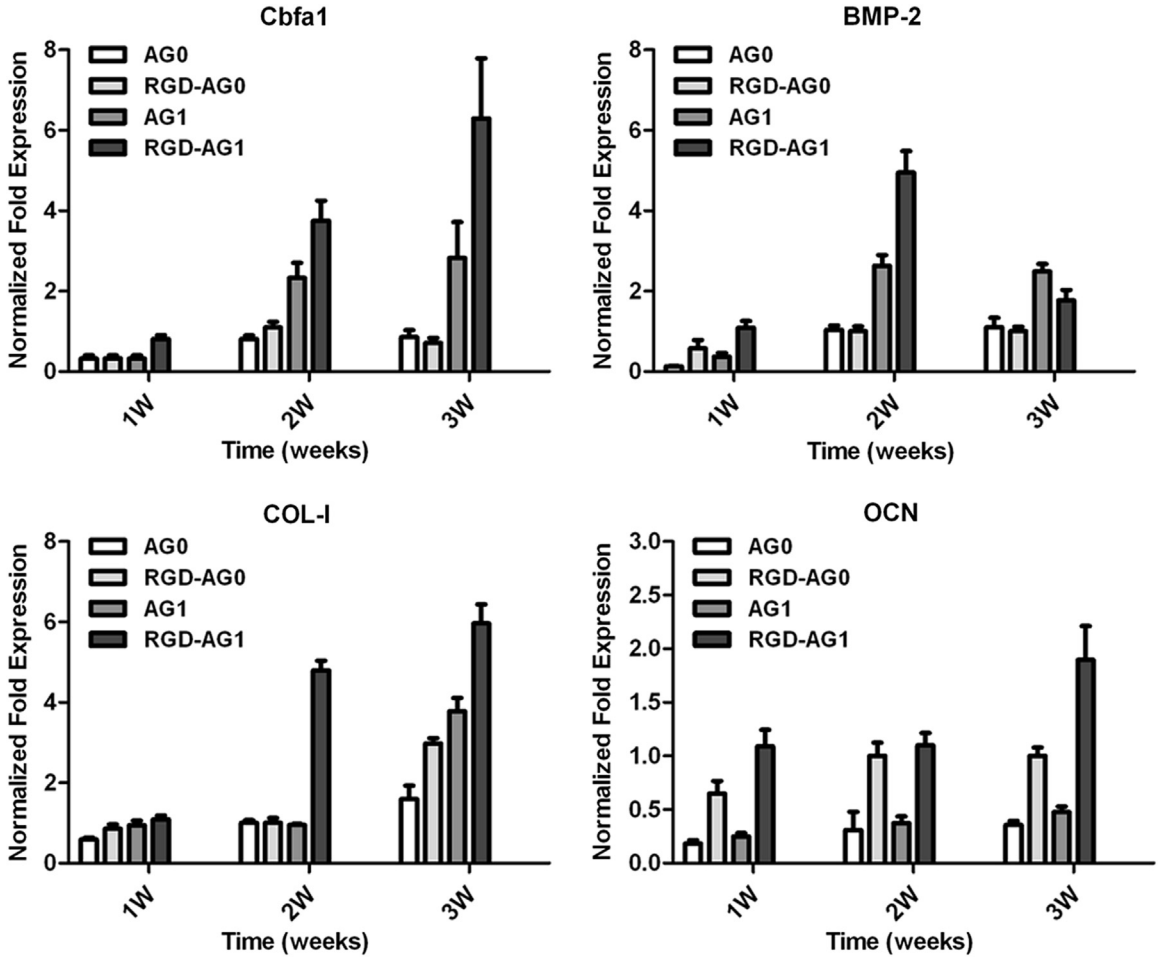

Fig. 8. Quantitative gene expressions of MG-63 cells cultured in various hydrogels after 1, 2 and 3 weeks by real-time RT-PCR. The expression levels were normalized to the expression of GAPDH as an internal control. The gene expressions of Cbfa1, COL-I and OCN in RGD-AG1 increased dramatically with the culture time and showed a statistically much higher level to other samples at the same time point, whereas the expression of BMP-2 was highest at week 2 and then down at week 3 ($^*p < 0.05$).

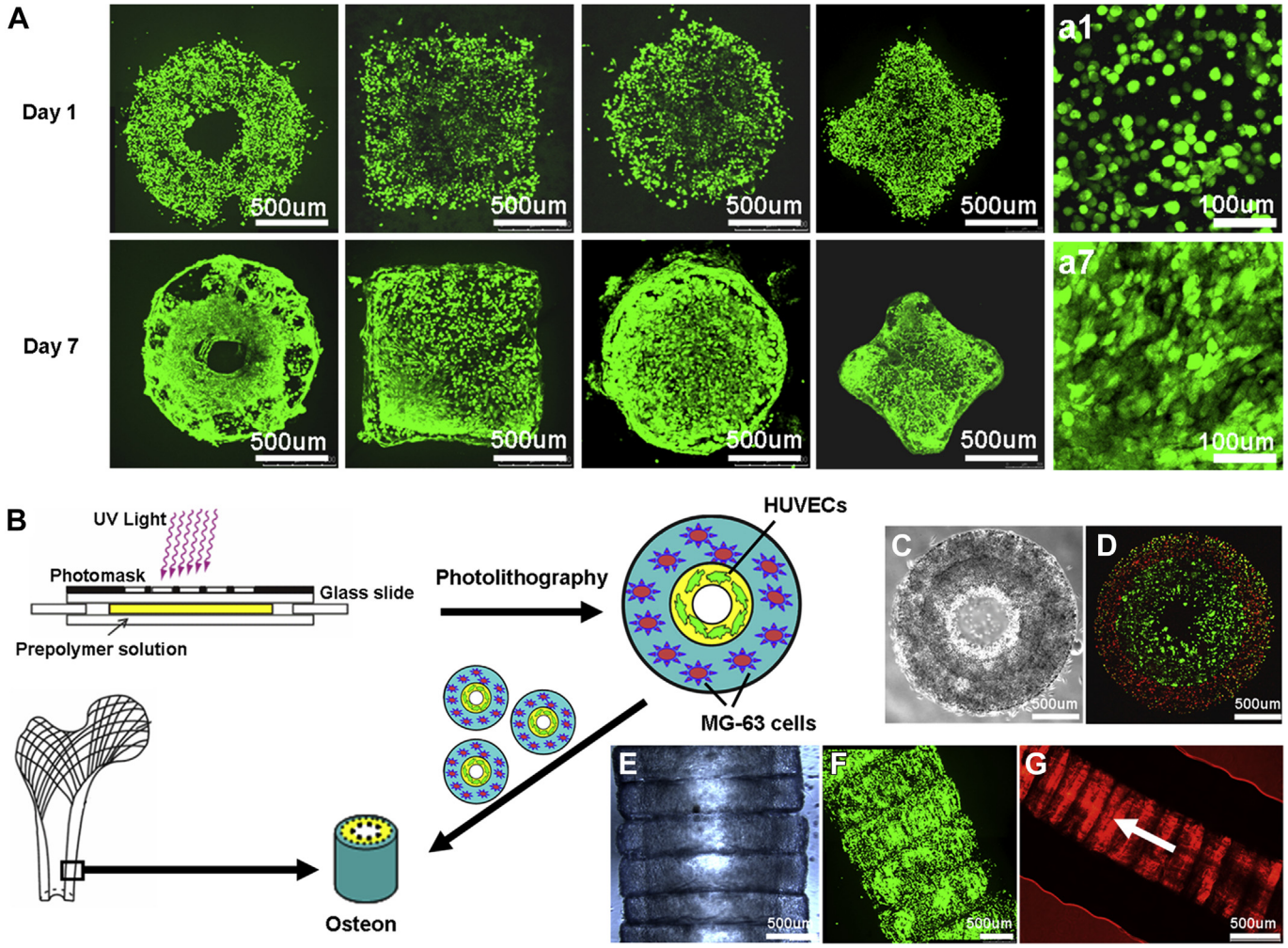

Fig. 9. (A) Confocal microscopy images of MG-63 cells encapsulated in microgels with shapes of ring, square, circle and cross respectively after 1 and 7 days by FDA/PI staining. The pictures a1 and a7 are the enlarged views of cellular morphology on day 1 and day 7, respectively. (B) Scheme for the construction of osteon-like structure. (C) Light image and (D) fluorescent image of double-layered circular microgel unit with HUVECs and MG-63 cells pre-labeled with green CMFDA and red CM-Dil cell trackers (Molecular Probes Inc., Eugene, OR), respectively. (E) Phase image and (F) confocal microscopy image of the hollow tubular osteon-like structure assembled by the double-ring microgels after culturing for 4 days by FDA/PI staining. (G) Fluorescent image of the osteon-like structure after perfusion test, and the white arrow represents the perfusion direction of Nile Red dye solution. (For interpretation of the references to color in this figure legend, the reader is referred to the web version of this article.)

affected the structural integrity of the hydrogel. Since a desirable mechanical property is vital to bone scaffolds, moreover, the integrity and stable appearance of micro-patterned scaffolds, relatively lower swelling ratio of hydrogels here, should be maintained when cultured in vitro, the amount of encapsulated gelatin was determined to be 1 mL gelatin per mL alginate. The next degradation experiment clearly showed that gelatin microspheres encapsulated in hydrogel gradually dissolute off at 37 °C to create cavities (Fig. 4), and the nearly complete degradation (90 ± 2%) after 3 days incubation also indicated the interconnected macroporosity in the material would be successfully achieved. Then, we chose human MG-63 osteoblasts to act as a model to evaluate the capacity of this adhesive macroporous hydrogel for cell adhesion, spreading as well as osteogenic differentiation. The MG-63 cell line derives from osteosarcoma represents an immature osteoblast phenotype and undergoes temporal development in long term culture, is commonly used as a model for osteoblast phenotype development and matrix mineralization [31]. In addition, it's a kind of anchorage-dependent cell, naturally in a spindle shape, so the stretched/spreading morphology is extremely important to its survival and function especially in osteogenic differentiation.

The high viability of encapsulated cells in all hydrogels as shown in Figs. 5 and 6A indicated the cytocompatible and non-toxic nature of these photocrosslinked alginate based hydrogels. As expected, the both incorporation of RGD and gelatin microspheres significantly promoted cell proliferation and spreading in the hydrogels (Fig. 6A, B). Cells around the microspheres began to spread first, then gradually grew into and eventually filled up the dissolution space as the microspheres gradually degraded. From day 1 to day 5, cells formed multiangular shape with protruding pseudopods gradually, and eventually developed a typical spindle shape. After that, the number of spread cells showed a continually increasing and direct cell–cell contact between spreading cells could be seen clearly. For an anchorage-dependent cell, the stretched morphology has a significant impact on cell–material interaction and determines the survival, adhesion, migration, differentiation and many other important behaviors of therapeutic cells. The successfully induced cell spreading in the adhesive macroporous hydrogels would provide fundamental support for the later osteogenic differentiation. While in hydrogels containing only RGD peptide or microspheres, cells proliferated slowly and the spreading was quite restricted even only several cell aggregations were formed. This

finding suggests that the successful cell spreading in the hydrogels requires not only cell-affinitive domains such as RGD, but also the creation of space to provide adequate room for cell migration/growth, and no one can be absent.

Alkaline phosphatase (ALP) activity, an early marker of osteogenesis [32], was firstly analyzed to evaluate the osteogenic differentiation of MG-63 cells in hydrogels (Fig. 7). ALP expression of cells in the RGD-AG1 and AG1 underwent the process of first increase at the early 2 weeks and then decrease at week 3, while that in the AG0 control remained at the original low level over the entire test period. For RGD-AG0, the ALP activity was highest on day 4 and then decreased with the culture. As it has been generally considered that the secretion of ALP increases before mineralization and decreases after the initiation of mineralization [32], the later decreased ALP expression indicated the initiation of mineralization of cells in these hydrogels whereas no mineralization occurred in the control because the ALP secretion remained low. Additionally, the significantly higher ALP expression level in RGD-AG1 also indicated a stronger mineralization compared with the other samples.

As markers of cell differentiation along the osteogenic linage, osteogenesis-related gene expressions were then assessed by qRT-PCR (Fig. 8). Gene expression in osteogenic differentiation can be divided into two stages. Genes involved in cell proliferation, migration and ECM synthesis are present at the early stages, whereas genes playing a role in maturation and mineralization are expressed at later stages of bone matrix formation [33]. Cbfa1 is an osteoblastic specific transcriptional factor which regulates osteogenesis marker gene differentiation and promotes bone formation [34]. Since it is the earliest osteogenic marker that activates the gene expression of ALP, OCN, and some other bone-specific proteins or enzymes, the significantly higher expression of cbfa1 in the RGD-AG1 indicated that a hydrogel containing both microspheres and RGD peptides was capable of up-regulating cbfa1 expression thus supporting adherent cell differentiation along the osteogenic lineage. The significantly higher expression of BMP-2 in RGD-AG1 at week 2 also proved this, since it is one of the genes encoding for a protein needed at early stages which can also activate osteogenic gene expression [32]. As BMP-2 was down-regulated during the following weeks, genes involved in mineralization and maturation, such as OCN, increased their expression at week 3 demonstrating phenotype maturation into osteoblast lineage. Besides, the dramatically high expression of COL-I, which is the major constituent of the native bone matrix and would provide the basic structural integrity of connective tissues for further mineralization, also reflected the enhancement of the progression of osteogenic differentiation after 2 weeks culturing in RGD-AG1 especially. As a later marker for osteogenesis, OCN plays a regulatory role in balancing the maintenance or resorption of bone mineralization [35]. Its generally low expression in all samples may be related to the short culturing period since OCN is a late marker of osteogenic differentiation only expressed by mature osteoblasts [36]. But the relatively higher expression in RGD-AG1 to some extent indicated the mineralization and maturing of cells in this hydrogel whereas less mineralization and differentiation occurred in other samples. In summary, the strongest presence of all these osteogenesis-related genes suggests enhanced ossification of MG-63 cells encapsulated in adhesive macroporous hydrogel RGD-AG1, with gene expression of markers relevant to multiple stages of osteogenesis. And the much higher expression of all genes in it also indicates much sharper promotion effect of osteogenic differentiation attributed to both the RGD peptide and gelatin microspheres.

As hypothesized in the beginning of this study, the successful spreading and enhanced osteogenic differentiation of MG-63 cells in RGD-AG1 hydrogel showed clearly the feasibility that cell function may be effectively enhanced by the simultaneous construction of cell-affinitive domains and sufficient spreading space in 3D hydrogel matrix. While in the pure alginate hydrogel AG0 and hydrogels only capable of cell affinity (RGD-AG0) or cell spreading space (AG1), cells could just exhibit either a rounded shape or a spreading morphology with a very limited degree, and the osteogenic differentiation was far beneath RGD-AG1. Besides, this photocrosslinkable hydrogel system which allows for spatial control over the polymerization reaction is particularly attractive for micro-tissue engineering enabling facile fabrication of complex 3D architectures. Microgels with different shapes, such as ring, square, circle and cross, were successfully fabricated. MG-63 cells in these micropatterned hydrogels, the original shapes of which were well kept, maintained a high activity and achieved a successful spreading after 7 days culture (Fig. 9A). Furthermore, complex structures can also be fabricated by the co-culturing multi types of cells with specific biorelevant functions in various shaped microgels to generate multiple microenvironments in scaffolds. Cortical bone, for example, is made up of cylindrical functional units called osteons which are composed of a Haversian canal that contain vasculature surrounded by several concentric lamellae of osteocytes [37]. Osteon can be constructed with spatially distributed osteocytes and HUVECs to mimic bone-like ECM and blood vessel-like micro tube in a scaffold respectively, and the assembly of these repeating osteon units would be seen as a simplified model of bone tissue [38–40]. A simple “double-ring” model designed here can simulate the osteon structure, and a hollow tubular structure with HUVECs laded in the inner layer and MG-63 cells laded in the outer layer was successfully assembled. As shown in Fig. 9B–G, the constructed osteon-like structure, constituted of two basic parts that played similarly essential roles in natural osteon (lamellae and Haversian canals), provided good living circumstances for cells. We hope to use this system to regenerate the basic structure of compact bone and investigate the HUVEC and osteocytes interaction to regulate the osteogenic function and vascularization of constructed bone grafts, thus promote the implant integration and vascularization.

5. Conclusions

The adhesive macroporous hydrogel model was developed to simultaneously construct cell-affinitive domains and sufficient spreading space for anchorage-dependent cells, so as to facilitate cell spreading and promote prolonged cell ingrowth, survival and differentiation. With the incorporation of gelatin microspheres, the hybrid alginate hydrogels exhibited significantly enhanced mechanical properties and decreased swelling ratios. The RGD peptide grafted on the alginate and the macropores generated by the dissolved gelatin microspheres influenced the MG63 cells shape and significantly enhanced their differentiation, as represented by the higher mRNA expression of Cbfa1, BMP-2, and COL-I as well as more ALP secretion. MG-63 cells in the adhesive macroporous alginate hydrogel showed the ability to overcome hydrogel enlacement and spread out into their native morphology, and the proliferation as well as osteogenic differentiation were greatly facilitated. Moreover, microgels with different shapes were fabricated, and micro-engineered complex structures constructed with spatially organized cell distribution and specific functions, such as osteon-like structure containing both osteogenic and vascularized area was successfully generated by a double-ring assembly. This is especially attractive in the bioengineering of tissues that have multiple cell types and require precisely defined cell–cell and cell–substrate interactions.

Acknowledgments

This work is supported by the National Natural Science Foundation of China (Contract Grant No. 51273121, 81071272, 51373105,

and 81190131) and National Basic Research Program of China (Contract Grant No. 2011CB606201).

References

[1] Liu Tsang V, Bhatia SN. Three-dimensional tissue fabrication. Adv Drug Deliv Rev 2004;56:1635–47.
[2] Griffith LG, Swartz MA. Capturing complex 3D tissue physiology in vitro. Nat Rev Mol Cell Biol 2006;7:211–24.
[3] Khetan S, Burdick JA. Patterning hydrogels in three dimensions towards controlling cellular interactions. Soft Matter 2011;7:830–8.
[4] Kloxin AM, Kloxin CJ, Bowman CN, Anseth KS. Mechanical properties of cellularly responsive hydrogels and their experimental determination. Adv Mater 2010;22:3484–94.
[5] Lutolf MP, Raeber GP, Zisch AH, Tirelli N, Hubbell JA. Cell-responsive synthetic hydrogels. Adv Mater 2003;15:888–92.
[6] Luo Y, Shoichet MS. A photolabile hydrogel for guided three-dimensional cell growth and migration. Nat Mater 2004;3:249–53.
[7] Khademhosseini A, Langer R, Borenstein J, Vacanti JP. Microscale technologies for tissue engineering and biology. Proc Natl Acad Sci U S A 2006;103:2480–7.
[8] Nelson CM, Tien J. Microstructured extracellular matrices in tissue engineering and development. Curr Opin Biotechnol 2006;17:518–23.
[9] Guillame-Gentil O, Semenov O, Roca AS, Groth T, Zahn R, Vörös J, et al. Engineering the extracellular environment: strategies for building 2D and 3D cellular structures. Adv Mater 2010;22:5443–62.
[10] DeForest CA, Polizzotti BD, Anseth KS. Sequential click reactions for synthesizing and patterning three-dimensional cell microenvironments. Nat Mater 2009;8:659–64.
[11] Khademhosseini A, Langer R. Microengineered hydrogels for tissue engineering. Biomaterials 2007;28:5087–92.
[12] Du Y, Lo E, Ali S, Khademhosseini A. Directed assembly of cell-laden microgels for fabrication of 3D tissue constructs. Proc Natl Acad Sci 2008;105:9522–7.
[13] Aubin H, Nichol JW, Hutson CB, Bae H, Sieminski AL, Cropek DM, et al. Directed 3D cell alignment and elongation in microengineered hydrogels. Biomaterials 2010;31:6941–51.
[14] Wang C, Varshney RR, Wang D-A. Therapeutic cell delivery and fate control in hydrogels and hydrogel hybrids. Adv Drug Deliv Rev 2010;62:699–710.
[15] Giancotti FG, Ruoslahti E. Integrin signaling. Science 1999;285:1028–33.
[16] Frisch SM, Ruoslahti E. Integrins and anoikis. Curr Opin Cell Biol 1997;9:701–6.
[17] Re F, Zanetti A, Sironi M, Polentarutti N, Lanfrancone L, Dejana E, et al. Inhibition of anchorage-dependent cell spreading triggers apoptosis in cultured human endothelial cells. J Cell Biol 1994;127:537–46.
[18] Guvendiren M, Burdick JA. The control of stem cell morphology and differentiation by hydrogel surface wrinkles. Biomaterials 2010;31:6511–8.
[19] Suri S, Schmidt CE. Photopatterned collagen–hyaluronic acid interpenetrating polymer network hydrogels. Acta Biomater 2009;5:2385–97.
[20] Sun J, Xiao W, Tang Y, Li K, Fan H. Biomimetic interpenetrating polymer network hydrogels based on methacrylated alginate and collagen for 3D preosteoblast spreading and osteogenic differentiation. Soft Matter 2012;8:2398–404.
[21] Lau TT, Wang C, Wang D-A. Cell delivery with genipin crosslinked gelatin microspheres in hydrogel/microcarrier composite. Compos Sci Technol 2010;70:1909–14.
[22] Wang C, Bai J, Gong Y, Zhang F, Shen J, Wang DA. Enhancing cell affinity of nonadhesive hydrogel substrate: the role of silica hybridization. Biotechnol Prog 2008;24:1142–6.
[23] Matsunaga YT, Morimoto Y, Takeuchi S. Molding cell beads for rapid construction of macroscopic 3D tissue architecture. Adv Mater 2011;23:H90–4.
[24] Gillette BM, Jensen JA, Wang M, Tchao J, Sia SK. Dynamic hydrogels: switching of 3D microenvironments using two-component naturally derived extracellular matrices. Adv Mater 2010;22:686–91.
[25] Liu Y, Chan-Park MB. Hydrogel based on interpenetrating polymer networks of dextran and gelatin for vascular tissue engineering. Biomaterials 2009;30:196–207.
[26] Sakai S, Ito S, Ogushi Y, Hashimoto I, Hosoda N, Sawae Y, et al. Enzymatically fabricated and degradable microcapsules for production of multicellular spheroids with well-defined diameters of less than 150μm. Biomaterials 2009;30:5937–42.
[27] Kloxin AM, Tibbitt MW, Kasko AM, Fairbairn JA, Anseth KS. Tunable hydrogels for external manipulation of cellular microenvironments through controlled photodegradation. Adv Mater 2010;22:61–6.
[28] Lau TT, Lee LQP, Vo BN, Su K, Wang D-A. Inducing ossification in an engineered 3D scaffold-free living cartilage template. Biomaterials 2012;33:8406–17.
[29] Su K, Lau TT, Leong W, Gong Y, Wang DA. Creating a living hyaline cartilage graft free from non-cartilaginous constituents: an intermediate role of a biomaterial scaffold. Adv Funct Mater 2012;22:972–8.
[30] Chou AI, Nicoll SB. Characterization of photocrosslinked alginate hydrogels for nucleus pulposus cell encapsulation. J Biomed Mater Res A 2009;91:187–94.
[31] Czekanska E, Stoddart M, Richards R, Hayes J. In search of an osteoblast cell model for in vitro research. Eur Cell Mater 2012;24:1–17.
[32] Lian JB, Stein GS. Concepts of osteoblast growth and differentiation: basis for modulation of bone cell development and tissue formation. Crit Rev Oral Biol Med 1992;3:269–305.
[33] Kärner E, Bäckesjö C-M, Cedervall J, Sugars RV, Ährlund-Richter L, Wendel M. Dynamics of gene expression during bone matrix formation in osteogenic cultures derived from human embryonic stem cells in vitro. Biochim Biophys Acta 2009;1790:110–8.
[34] Ducy P, Zhang R, Geoffroy V, Ridall AL, Karsenty G. Osf2/Cbfa1: a transcriptional activator of osteoblast differentiation. Cell 1997;89:747–54.
[35] Jundt G, Berghäuser K-H, Termine J, Schulz A. Osteonectin—a differentiation marker of bone cells. Cell Tissue Res 1987;248:409–15.
[36] Owen TA, Aronow M, Shalhoub V, Barone LM, Wilming L, Tassinari MS, et al. Progressive development of the rat osteoblast phenotype in vitro: reciprocal relationships in expression of genes associated with osteoblast proliferation and differentiation during formation of the bone extracellular matrix. J Cell Physiol 1990;143:420–30.
[37] Rho JY, Kuhn-Spearing L, Zioupos P. Mechanical properties and the hierarchical structure of bone. Med Eng Phys 1998;20:92–102.
[38] Hofmann T, Heyroth F, Meinhard H, Fränzel W, Raum K. Assessment of composition and anisotropic elastic properties of secondary osteon lamellae. J Biomech 2006;39:2282–94.
[39] Chen X, Ergun A, Gevgilili H, Ozkan S, Kalyon DM, Wang H. Shell-core bi-layered scaffolds for engineering of vascularized osteon-like structures. Biomaterials 2013;34:8203–12.
[40] Zuo Y, Xiao W, Chen X, Tang Y, Luo H, Fan H. Bottom-up approach to build osteon-like structure by cell-laden photocrosslinkable hydrogel. Chem Commun 2012;48:3170–2.